American Mineralogist, Volume 61, pages 549–559, 1976

Temperatures in the mantle as inferred from simple compositional models

E. K. GRAHAM AND D. DOBRZYKOWSKI

Department of Geosciences and Materials Research Laboratory
The Pennsylvania State University, University Park, Pennsylvania 16802

Abstract

Recent very high-pressure phase-equilibria experiments (*e.g.* Kumazawa *et al.*, 1974; Ming and Bassett, 1975) have indicated that the olivine and spinel forms of $(Mg,Fe)_2SiO_4$ transform into an assemblage of the oxides (Mg,Fe)O (NaCl structure) plus SiO_2 (stishovite) in a pressure and temperature regime which corresponds to the 650 km seismic discontinuity of the mantle. This investigation tests the mixed-oxide model against the elastic and density requirements of the mantle within the region immediately below the 650 km discontinuity (approximately 650 to 1200 km). Mixed-oxide compositions containing combinations of (Mg,Fe)O and SiO_2 which correspond to dunite–peridotite and pyroxenite were emphasized in the modelling procedure. Models in the compositional range dunite–peridotite were found to satisfy the *P* and *S*-wave velocities, as well as the density requirements below the 650 km discontinuity; satisfactory solutions were provided by such models when $Fe/(Mg+Fe) = 0.15 \pm 0.05$ along an adiabatic temperature gradient of 1300°C at zero pressure. Models of pyroxenite composition do not satisfy the physical properties of the mantle in the region of interest.

The successful dunite–peridotite mixed-oxide compositional models provide an estimate of the geotherm in the 650–1200 km region of the mantle. Since the physical properties within the region of interest are satisfied along an adiabat, the problem is reduced to calculating the increase of temperature with depth for the preferred model along the adiabatic gradient (initial temperature 1300°C). This procedure yields a geotherm which is consistent with several independent upper mantle temperature estimates. The present results indicate a temperature of 1600 ± 400°C at 671 km; the primary source of uncertainty is the accuracy of the seismic model interpretations.

Introduction

Although surface heat flow and related data provide some indication of the temperature distribution within the crust and topmost upper mantle, at depths in excess of perhaps 50 km temperature becomes increasingly difficult to evaluate within a desirable degree of uncertainty. Because it cannot be measured directly below deep drillholes, temperature must be inferred from physical or compositional properties which characterize the region of interest. For example, temperature estimates for the mantle have been calculated on a basis of electrical conductivity (Tozer, 1959; Bell and Mao, 1975; Duba *et al.*, 1975), density and elastic properties (Anderson, 1967; Fujisawa, 1968; Graham, 1970; Wang, 1972), experimental and theoretical melting relations (Uffen, 1952; Clark and Ringwood, 1964), as well as from experimental temperatures and pressures of equilibration of coexisting minerals from kimberlite xenoliths and ultramafic inclusions in basalts (Boyd, 1973; MacGregor and Basu, 1974). Each method, of course, is not without its assumptions and accompanying ambiguities. The most satisfactory geotherms are those which are based on models that provide self-consistent explanations for the greatest number of geophysical and petrological constraints.

It is the purpose of this investigation to assess the fundamental composition of the mantle in the region immediately below the 650 km seismic discontinuity; and in addition, to infer the temperature distribution in this zone on a basis of compositional models which are found to be satisfactory. The fundamental criterion for a successful compositional model is consistency with the density and seismic velocity requirements within the relevant depth range. Of all the properties which characterize the internal constitution of earth below the crustal layer, the distribution

of the *P*- and *S*-wave velocities as functions of depth are known with the greatest degree of accuracy. It is therefore fitting that they should provide the primary constraint in evaluating compositional models of the deep interior.

Compositional and seismic models

In the present study, three simple hypothetical model compositions were selected for testing in comparison to the geophysical constraints:

Model A: $2(Mg,Fe)O + SiO_2$
Model B: $5(Mg,Fe)O + 3SiO_2$
Model C: $(Mg,Fe)O + SiO_2$

where (Mg,Fe)O corresponds to the magnesiowustite solid solution (NaCl structure) and SiO_2 refers to stishovite (rutile structure); the component fractions are molar. Clearly, each model provides for variation in iron content [Fe/(Mg+Fe)ratio]; moreover, consideration of all three models allows an evaluation of the SiO_2 content relative to (Mg,Fe)O. Support for the foregoing basic compositions as appropriate primary models is provided by petrological, high-pressure phase equilibria, and elastic property data.

The composition of the upper mantle is discussed frequently in terms of the primary essential mineral components olivine, pyroxene, and garnet (and perhaps amphibole in some restricted regions). There are, of course, two principal ultramafic rock types which contain these minerals, peridotite (olivine–pyroxene) and eclogite (pyroxene–garnet). The hypothesis that the upper mantle is composed dominantly of either of these rock types (most geoscientists tend to favor the dunite-peridotite family) is supported by the occurrence and significance of Alpine peridotites, and the compositions of kimberlite xenoliths and ultramafic nodules in basalts (*e.g.* Ringwood, 1966; Fujisawa, 1968; McGetchin and Silver, 1970). Moreover, it has been shown by several investigators (*e.g.* Anderson, 1967; Graham, 1970; Ahrens, 1972, 1973) that dunite–peridotite type rocks have the requisite physical properties to satisfy the geophysical constraints within the upper mantle. Models A through C are representative of the basic chemical compositions (in terms of the $MgO–FeO–SiO_2$ ternary system) of dunite, peridotite, and pyroxenite. The model compositions are compared with real rock averages in Table 1.

TABLE 1. Model chemical compositions in comparison to average rock analyses (weight percentage)

Component	Dunite[1]	A	Peridotite[2]	B	Eclogite[3]	C
SiO_2	41.3	40.9	43.5	45.3	49.0	58.0
MgO	49.8	49.3	34.0	45.6	8.9	35.0
FeO[4]	7.1	9.8	10.3	9.1	12.9	6.9
CaO	--	--	3.5	--	11.5	--
Al_2O_3	0.5	--	4.0	--	14.5	--
Others[5]	--	--	2.8	--	3.2	--

1. Green and Ringwood (1963)
2. Nockolds (1954)
3. Lapadu-Hargues (1953)
4. Models calculated on a basis of $(Mg_{0.90}, Fe_{0.10})O$; rock analyses include Fe_2O_3
5. Principally Na_2O, K_2O, TiO_2, MnO, H_2O, and P_2O_5

As indicated in Table 1, the model compositions differ from the real rock analyses chiefly in terms of CaO and Al_2O_3. The degree to which the model "rocks" are representative of the indicated rock types must be evaluated in terms of their respective elastic properties. Since the averages of the relevant elastic properties (bulk modulus K and rigidity μ) for CaO and Al_2O_3 are in the neighborhood of those for (Mg,Fe)O, the dunite and peridotite models are undoubtedly satisfactory. The eclogite analysis in Table 1 differs more significantly from the model pyroxenite in terms of basic oxide components. For this reason, an "oxide" model for this rock should include the Al_2O_3 and CaO fractions. The occurrence of other minor chemical components in the real rock types has a negligible effect on the bulk elastic properties.

Numerous recent interpretations of the seismic *P*-wave velocity-depth profiles in the transition zone of the mantle demonstrate the occurrence of two distinct "steps" or second-order discontinuities in the regions of 400 and 650 km depth (*e.g.*, Niazi and Anderson, 1965; Johnson, 1967; Archambeau *et al.*, 1969). These discontinuities, following the suggestion of Birch (1952), are inferred to represent the increases in velocity induced by phase transitions in ferromagnesian silicates from their low-pressure upper-mantle modifications, to lower-mantle close-packed structural forms. High-pressure and high-temperature phase-equilibria studies, principally by Ringwood and Major (1966) and Akimoto and Fujisawa (1968), have indicated that the upper discontinuity at 400 km correlates with the transformation of olivine, $(Mg,Fe)_2SiO_4$, into the β- or γ-spinel structure. In addition, recent very high pressure experiments have begun to disclose the nature of the spinel–post-spinel transition near 650 km. Bassett and Takahashi (1970) observed that Fe_2SiO_4 (spinel) disproportionates into FeO plus SiO_2 (stishovite) when subjected to pressures of about 250 kbar in a diamond anvil cell; the

sample was heated simultaneously with a light beam from a pulsed ruby laser. Later work by Kumazawa *et al.* (1974) and Ming and Bassett (1975) indicates that olivine and spinel samples throughout the entire range of Mg–Fe solid solution disproportionate into (Mg,Fe)O (NaCl structure) plus SiO_2 (stishovite) within the pressure and temperature range of the 650 km seismic discontinuity. This work clearly has provided the motivation to assess the physical properties of the region of the mantle immediately below the 650 km discontinuity in terms of basic mixed-oxide compositional models.

In this study, the elastic properties and density of the mantle are assumed to be given by Jordan's (1973) inversion model B1. This model was constructed in such a manner that it satisfies an extensive set of fundamental spheroidal and torsional mode eigenperiods, as well as differential and absolute travel-time data. It is assumed, for purposes of testing the various compositional models under present consideration, that those models which have density and seismic velocity profiles in the region of interest that correlate with those of B1 are acceptable solutions. Obviously, if the physical properties of a given compositional model are consistent with B1, then that composition satisfies the geophysical constraints of the B1 data set. In order to allow for an appropriate margin of error in the seismic velocity profiles, and thus provide a semi-quantitative criterion for establishing "satisfactory" solutions, the extremal inversion uncertainty bounds for velocity structure in the mantle derived by Wiggins *et al.* (1973) were used in conjunction with the B1 model results. The final test for an acceptable compositional model, in terms of the geophysical requirements, is a density profile over the region of interest within ±1 percent of that of model B1 (this uncertainty in the density of the mantle follows the suggestion of Wang, 1972), and *P*- and *S*-wave velocities which fall within the Wiggins *et al.* (1973) envelopes (the B1 profiles fall well within these bounds).

Elastic properties of the compositional models at very high pressure and temperature

The compositional models proposed in this investigation were tested against model B1 within the region of interest by direct comparison of the *P*- and *S*-wave velocities and density. In order to calculate the relevant properties at the pressure and temperature conditions prevailing within the sub-transition zone, the usual finite strain equations of state (Birch, 1939; Sammis *et al.*, 1970) were used, complete to third order in the expansion of the Eulerian strain energy. The pertinent expressions for the pressure P and adiabatic bulk modulus K^S, as functions of density ρ, are as follows:

$$P(\rho) = \tfrac{3}{2} K_0{}^S[(\rho/\rho_0)^{7/3} - (\rho/\rho_0)^{5/3}] \cdot\left\{1 - \frac{3}{4}\left[4 - \left(\frac{\partial K^S}{\partial P}\right)_{S,0}\right][(\rho/\rho_0)^{2/3} - 1]\right\} \quad (1)$$

and

$$K^S(\rho) = K_0{}^S(\rho/\rho_0)^{5/3}\left\{1 + \tfrac{1}{2}[(\rho/\rho_0)^{2/3} - 1] \cdot\left[3\left(\frac{\partial K^S}{\partial P}\right)_{S,0} - 5\right]\right\} \quad (2)$$

where the subscript or superscript S denotes the adiabatic value of the elastic constant, and subscript 0 indicates the value of the parameter at zero pressure. Notice that the only experimental material properties required are ρ_0, $K_0{}^S$, and $(\partial K^S/\partial P)_{S,0}$; in the above forms, these equations generate curves for P and $K^S(P)$ along an adiabatic temperature profile. Finite strain theory also provides equations for the *P*- and *S*-wave velocities which take the form

$$V_P{}^2(\rho) = \frac{1}{\rho}(\rho/\rho_0)^{5/3}\{K_0{}^S + \tfrac{4}{3}\mu_0 + \tfrac{1}{2}[(\rho/\rho_0)^{2/3} - 1](11K_0{}^S + \tfrac{8}{3}\mu_0 - \zeta)\}, \quad (3)$$

where

$$\zeta = K_0{}^S\left[16 - 3\left(\frac{\partial K^S}{\partial P}\right)_{S,0} - 4\left(\frac{\partial \mu}{\partial P}\right)_0\right] + \frac{28}{3}\mu_0, \quad (4)$$

and

$$V_S{}^2(\rho) = \frac{1}{\rho}(\rho/\rho_0)^{5/3}\{\mu_0 + \tfrac{1}{2}[(\rho/\rho_0)^{2/3} - 1] \cdot(3K_0{}^S + 2\mu_0 + \eta)\} \quad (5)$$

where

$$\eta = 3K_0{}^S\left[\left(\frac{\partial \mu}{\partial P}\right)_0 - 1\right] - 7\mu_0. \quad (6)$$

In the foregoing relations μ denotes the rigidity modulus; the material properties μ_0 and $(\partial\mu/\partial P)_0$ constitute the only additional required experimental parameters. Since the pressure over the range of interest in the present study never exceeds 500 kbar, roughly one-quarter of the compositional model bulk modulus, the above third-order equation of state forms generate curves of sufficient accuracy for comparison with the seismic interpretations.

The finite strain equations determine, in effect, the

bulk modulus, and the P- and S-wave velocities, as functions of pressure along an adiabat which is initiated at a temperature T_0. The initial or zero pressure temperature T_0 may vary, provided that the experimental input material properties are evaluated accordingly. In order to calculate adiabatic curves for the necessary properties at elevated temperatures the following relations were used:

$$\rho_0(T_0) = \rho_0(25°C)\,(1 - \alpha\Delta T), \tag{7}$$

$$K_0{}^S(T_0) = K_0{}^S(25°C) + \left(\frac{\partial K^S}{\partial T}\right)_{S,0} \Delta T \tag{8}$$

and

$$\mu_0(T_0) = \mu_0(25°C) + \left(\frac{\partial \mu}{\partial T}\right)_0 \Delta T \tag{9}$$

where $\Delta T = T_0 - 25°C$. Because of the lack of relevant data, the pressure derivatives of the elastic properties appearing in equations (1) through (6) were assumed to be independent of temperature. As suggested by equations (7) through (9), additional experimental material properties are required; these include the volume thermal expansion coefficient α, and the temperature derivatives of K^S and μ, evaluated at zero pressure.

The elastic properties of compositional models, A, B, and C were derived on a basis of combinations of the fundamental oxide components MgO, FeO, and SiO_2. In addition, the elasticity of the magnesiowustite solid solution (Mg,Fe)O was assumed to follow a linear dependence between the two end-members. Table 2 lists the pertinent elastic property data used in the investigation. The MgO and FeO measurements were carried out using ultrasonic methods on single-crystal and polycrystal samples, respectively. Pressure and temperature data are not, at present, available for FeO; the required values were assumed to be equivalent to those of MgO. Because the compositions of interest are magnesium-rich, the uncertainty introduced by this supposition is not of significant concern. The data for stishovite were based on the results of a recent lattice theoretical model by Striefler and Barsch (1975) augmented by shock-wave experimental data.

TABLE 2. The elastic property and auxillary data for the basic oxides MgO, FeO, and SiO_2 (stishovite). (Superscripts indicate the source of the data.)

Property	MgO	FeO	SiO_2	Units
ρ_o	3.584[1]	5.948[2]	4.287[3]	gm/cm^3
K_o^S	1622[1]	1655[2]	3145[3]	Kbar
μ_o	1308[1]	557[2]	2030[3]	Kbar
$(\partial K^S/\partial P)_o$	4.28[1]	--	7.0[3]	--
$(\partial \mu/\partial P)_o$	2.14[1]	--	1.13[3]	--
$(\partial K^S/\partial T)_o$	-0.16[4]	--	-0.35[5]	Kbar/°C
$(\partial \mu/\partial T)_o$	-0.23[4]	--	-0.16[6]	Kbar/°C
α	$31.5(10^{-6})$[7]	$37.5(10^{-6})$[8]	$18(10^{-6})$[9]	$°C^{-1}$
Cp	$9.25(10^{-3})$[10]	$7.20(10^{-3})$[11]	$7.15(10^{-3})$[12]	$\frac{Kbar\ cm^3}{gm°C}$

1. Chang and Barsch (1969)
2. Mitzutani et al (1972) (approximately $Fe_{0.98}O$)
3. Striefler and Barsch (1975)
4. Anderson and Andreatch (1966)
5. Graham (1973)
6. Inferred from the isostructural oxides GeO_2, TiO_2, and SnO_2
7. White and Anderson (1966)
8. Calculated from data in Handbook of Physical Constants (1966)
9. Weaver et al (1973)
10. Victor and Douglas (1963)
11. Calculated from enthalpy data in Robie and Waldbaum (1968)
12. Holm et al (1967)

The stishovite data in Table 2 warrant some additional remarks. Compositional aspects of the lower mantle have been discussed and evaluated previously in terms of mixed-oxide models; notable in this regard are the studies by Fujisawa (1968), Anderson and Jordan (1970), and Davies (1974). However, due to the lack of shear-wave data and pressure or temperature measurements, these investigations were limited to modelling in terms of bulk modulus and density only. The data for SiO_2 used in this study were calculated recently by Striefler and Barsch (1975) using a modified rigid ion lattice dynamical model. In their theoretical approach, the usual Coulomb interaction among the ions and short-range repulsion between silicon–oxygen and oxygen–oxygen ions are included, as well as special angle bending forces to account for the oxygen–silicon–oxygen interaction. Deviations from purely ionic bonding were approximated by introducing an empirical scaling parameter for the ionic charges. Determination of the relevant force constants was afforded by a simultaneous least-squares fit involving experimental data for the elastic constants and Raman and IR frequencies for the isostructural oxides GeO_2 and SnO_2, and two IR frequencies for SiO_2 (stishovite). Figure 1 shows the values of K, μ, and the ratio K/μ for stishovite from the theoretical lattice model, in comparison to similar values for the isostructural (rutile structure) oxides GeO_2, TiO_2, and SnO_2. The consistency of the Striefler and Barsch results with the single-crystal experimental data is clear. In contrast, experimental results for polycrystal stishovite by Chung (1973) and Mitzutani *et al.* (1972) are also indicated on Figure 1. Because of the inconsistencies between these values

and the other rutile structure data, the lattice theory predictions were considered the most reliable.

Lastly, in order to model the bulk elastic properties of the isotropic polycrystal aggregate of (Mg,Fe)O (magnesiowustite) plus SiO_2 (stishovite), it is necessary to combine the individual mineral values in an appropriate manner. For this purpose, we used the usual VRH averaging scheme (Hill, 1952) for all calculations. As pointed out by Thomsen (1972), the "VRH average" is without theoretical justification; however, it has been effective empirically in predicting the isotropic aggregate moduli from single-crystal data for many silicates and oxides of geologic interest. Moreover, in many cases the VRH scheme yields aggregate property values which are quite close to those predicted by the more rigorous theory of Kröner (1967). For the present situation, Thomsen (1972) has shown that the seismic parameter $\Phi_0 = K_0/\rho_0$ of a mixture of stishovite, wustite, and MgO, as determined by the Kröner method, differs from the "VRH average" by less than 1 percent. Thus, the latter has some theoretical support for use in the "mixed-oxide" problem. We prefer the VRH scheme on a basis of ease of application.

Calculations for the compositional models and results

The testing procedure for the various compositional models follows three straight-forward steps. Initially, an adiabat is selected for the model under consideration by comparing directly calculated bulk-modulus profiles at several elevated temperatures with $K(P)$ as defined by Jordan's (1973) inversion model B1. This step is facilitated by the fact that the bulk modulus for a particular model (*i.e.* A,B, or C) is nearly independent of Fe-content. The most appropriate adiabat initial temperature may therefore be determined by interpolation. Figure 2 indicates the method and results for compositional Model A over the sub-transition zone range of interest. In this case, calculations were performed for the magnesium end member ($2MgO+SiO_2$) only, since $K(P)$ is not appreciably affected by the addition of iron. Adiabats were generated at initial temperatures of 25, 1000, and 2000°C; on this basis, an adiabat of 1100°C was selected as providing the best fit to model B1 over the appropriate pressure range.

Having determined a suitable adiabat initial temperature for a given compositional model, a similar procedure was applied in order to assess the most appropriate Fe/(Mg+Fe) fraction. This was accomplished by comparing several density profiles, calculated along the predetermined adiabat, with the density distribution of model B1. Initial density was varied by altering the Fe/(Mg+Fe) in the magnesiowustite mineral component of the model. The results of this procedure for compositional Model A (dunite) are shown in Figure 3. Adiabats at an initial temperature of 1100°C were generated for Fe/(Mg+Fe) ratios of 0.60, 0.80, and 1.00. Direct comparison with B1 indicates that the appropriate ratio for Model A (dunite) is about 0.15. At this point, the initial zero-pressure temperature and iron content which provide the closest "fit" to the $\rho(P)$ and $K(P)$ profiles of B1 have been determined for the given compositional model.

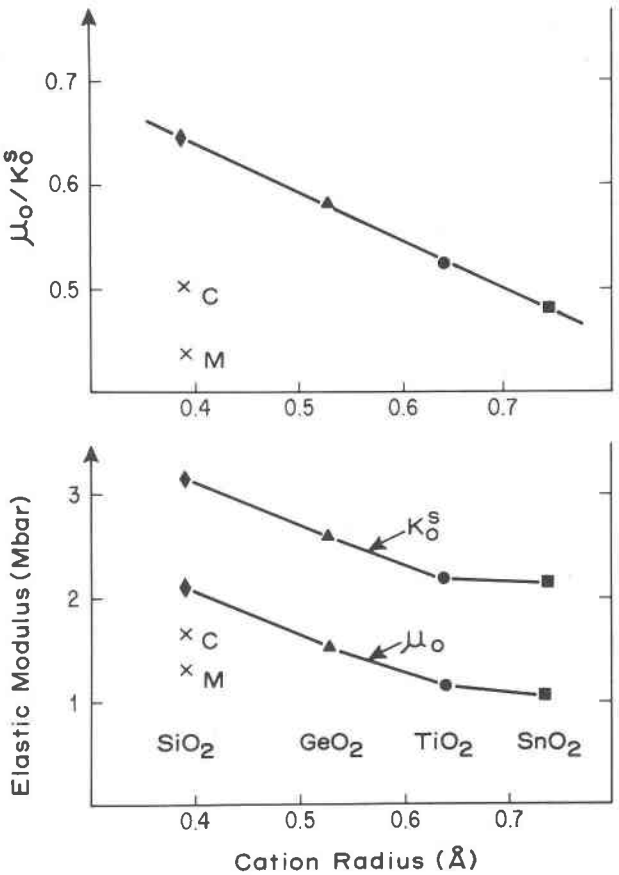

FIG. 1. Systematic behavior between the elastic properties and cation radius for SiO_2 (stishovite) and other single-crystal rutile structure oxides (TiO_2, Manghnani, 1969; GeO_2, Wang and Simmons, 1973; SnO_2, Chang and Graham, 1975). The data marked *C* and *M* represent polycrystal experimental values by Chung (1973) and Mitzutani *et al.* (1972).

Lastly, a direct comparison was made between the compositional model under consideration, along the adiabat and with the Fe-content determined by the foregoing procedure, and Jordan's inversion model B1; this final check includes the *P*- and *S*-wave veloci-

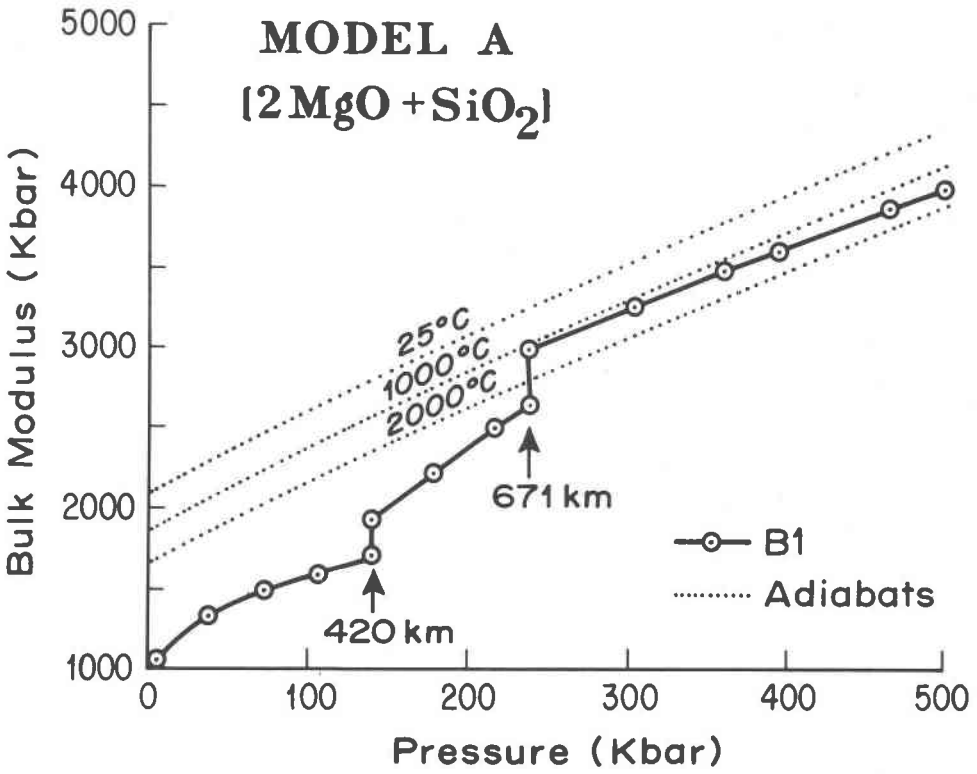

FIG. 2. Three calculated adiabats for the bulk modulus of compositional Model A (dunite) compared with $K(P)$ in earth's interior, as represented by inversion model B1 (Jordan, 1973).

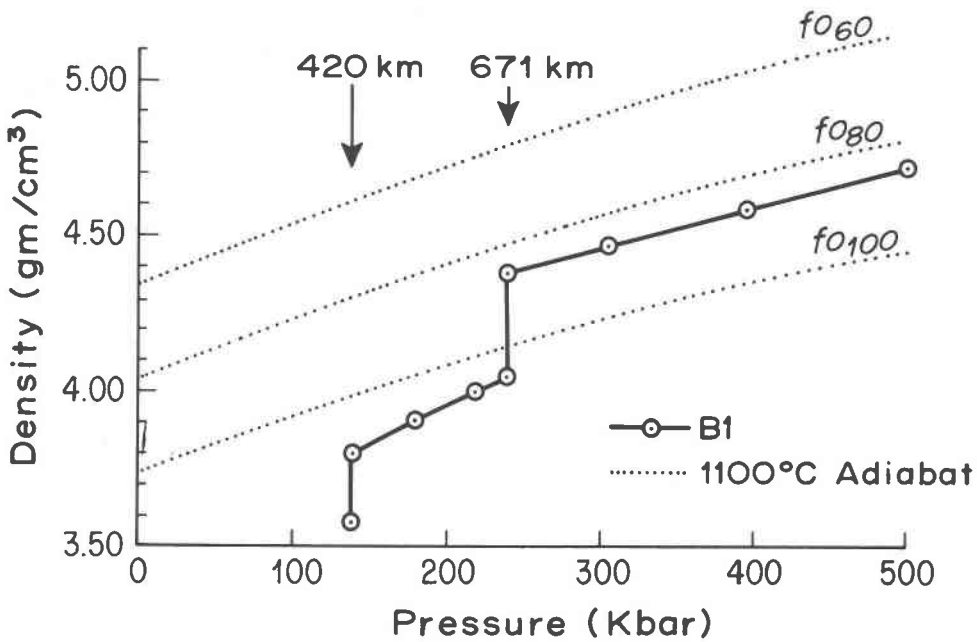

FIG. 3. Three calculated 1100°C zero-pressure adiabats for compositional Model A (dunite) in comparison to $\rho(P)$ from model B1 (Jordan, 1973). The profiles correspond to Fe/(Mg+Fe) of 1.00 ($f_{o_{100}}$), 0.80 ($f_{o_{80}}$), and 0.60 ($f_{o_{60}}$).

ties, as well as density and bulk modulus. A "satisfactory" compositional model must demonstrate physical properties which correspond to those of B1 within the bounds as defined by Wiggins *et al.* (1973) for the seismic velocities, and the limits indicated previously for density and bulk modulus. The final results for Model A (dunite) are shown in Figure 4. This model provides an excellent fit to all requirements when an Fe/(Mg+Fe) ratio of 0.15 is used along an 1100°C adiabat.

An exactly analogous procedure was followed in order to evaluate Model B (peridotite) and Model C (pyroxenite) in terms of the physical properties of the sub-transition zone. The results for Model B are indicated in Figure 5. This composition also provides a set of physical properties which are consistent with those within the region of interest. In this case, the bulk modulus and density requirements are satisfied by a composition with an iron–magnesium ratio of 0.15, and an initial zero-pressure temperature of 1300°C for the adiabat. Thus, the foregoing analysis indicates that a composition in the range of dunite to peridotite, when the primary mineral phases are in the form of a mixture of the oxides (Mg,Fe)O (NaCl structure) and SiO_2 (stishovite), provides the elastic and density properties which are required within the region of the mantle immediately below the 650 km seismic discontinuity.

Figure 6 shows the results for Model C (pyroxe-

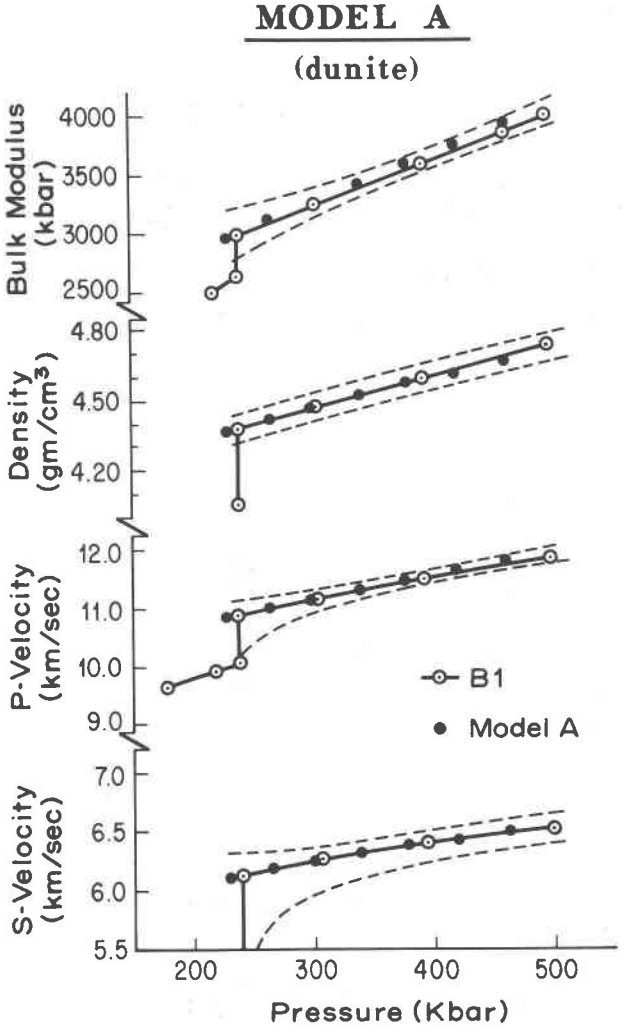

FIG. 4. Profiles for V_p, V_s, K, and ρ as calculated for compositional Model A at Fe/(Mg+Fe) equal to 0.15 along an 1100°C adiabat; the curves are shown in comparison to those of inversion model B1 (Jordan, 1973). The "bounds" (dashed lines) for a satisfactory fit are explained in the text.

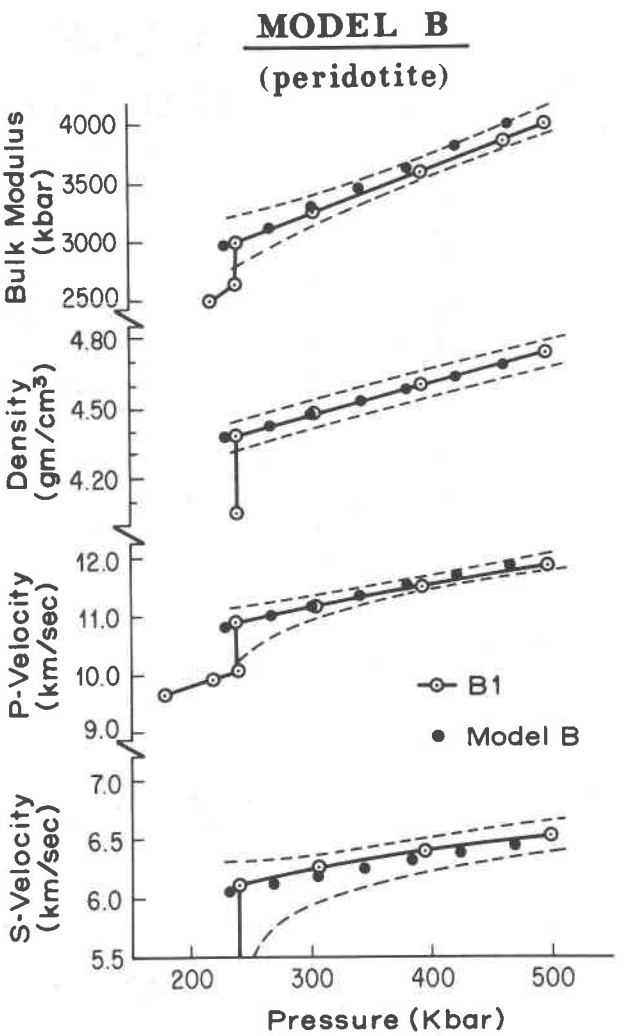

FIG. 5. Elastic property and density profiles for compositional Model B compared with inversion model B1 (Jordan, 1973). The Fe/(Mg+Fe) ratio is 0.15, and the adiabat initiates at 1300°C.

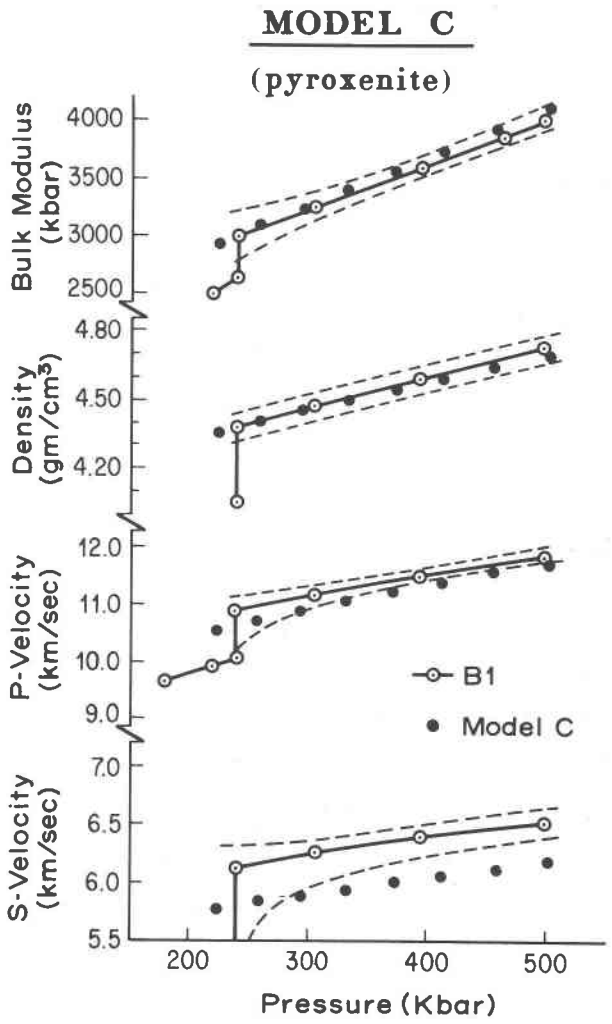

FIG. 6. Seismic and density profiles for Model C (pyroxenite) compared with inversion model B1 (Jordan, 1973). The compositional model was calculated on a basis of Fe/(Mg+Fe) equals 0.17, and an adiabat initiated at a temperature of 2300°C.

nite). Satisfactory correlation between the compositional model and seismic requirements for density and bulk modulus were obtained with Fe/(Mg+Fe) equal to 0.17 and an adiabat of 2300°C. However, these values produce *P*- and *S*-wave profiles which are not consistent with the seismic model bounds over much of the region of interest. For this reason, it does not appear that a mixed-oxide model with an $(Mg,Fe)O/SiO_2$ ratio as low as 1:1 provides a satisfactory solution to the sub-transition zone; in contrast, the dunite and peridotite models demonstrate that an $(Mg,Fe)O/SiO_2$ ratio of about 2:1 is more likely for this region of the mantle.

Temperatures within the sub-transition zone

In addition to evaluating the compositional aspects of the mantle within the region below the 650 km seismic discontinuity in terms of the mixed-oxide model, the foregoing analyses have demonstrated that the temperature gradient in the zone of interest probably does not deviate appreciably from the adiabatic. Thus, an estimate of the temperature distribution within the sub-transition region is provided by evaluating the adiabat for each of the compositional models, A, B, and C.

The temperature along an adiabat was calculated in the following manner. After combining Maxwell's thermodynamic relations with the definitions of the volume thermal expansion α and heat capacity at constant pressure C_p, it may be demonstrated that the adiabatic temperature–pressure gradient is given by

$$\left(\frac{\partial T}{\partial P}\right)_S = \alpha T/\rho C_p. \tag{10}$$

Moreover, since the thermal Grüneisen parameter γ is defined as

$$\gamma = \alpha K^S/\rho C_p, \tag{11}$$

equation (10) may be written in the form

$$\left(\frac{\partial T}{\partial P}\right)_S = \gamma T/K^S, \tag{12}$$

where K^S may be evaluated on the adiabat as a function of volume or pressure by equations (1) and (2). The variation of the volume dependent Grüneisen parameter on the adiabat was represented by the empirical relation (Ahrens *et al.*, 1970)

$$\gamma = \gamma_0(\rho_0/\rho)^A \tag{13}$$

where γ_0 is defined by equation (11) using the appropriate 25°C, zero pressure properties (γ is assumed to be independent of temperature over the range of interest). Graham (1973) has demonstrated that to first-order in compression, the exponent in equation (12) may be given by

$$A \cong \gamma_0 - \frac{1}{\alpha K^S}\left(\frac{\partial K^S}{\partial T}\right)_P - \left(\frac{\partial K^S}{\partial P}\right)_T + 1 \tag{14}$$

where again, the relevant parameters are evaluated at 25°C, zero pressure. Combining equations (12) and (13), the temperature gradient along the adiabat is given by

$$\left(\frac{\partial T}{\partial P}\right)_S = \frac{\gamma_0 T}{K^S}(\rho_0/\rho)^A. \tag{15}$$

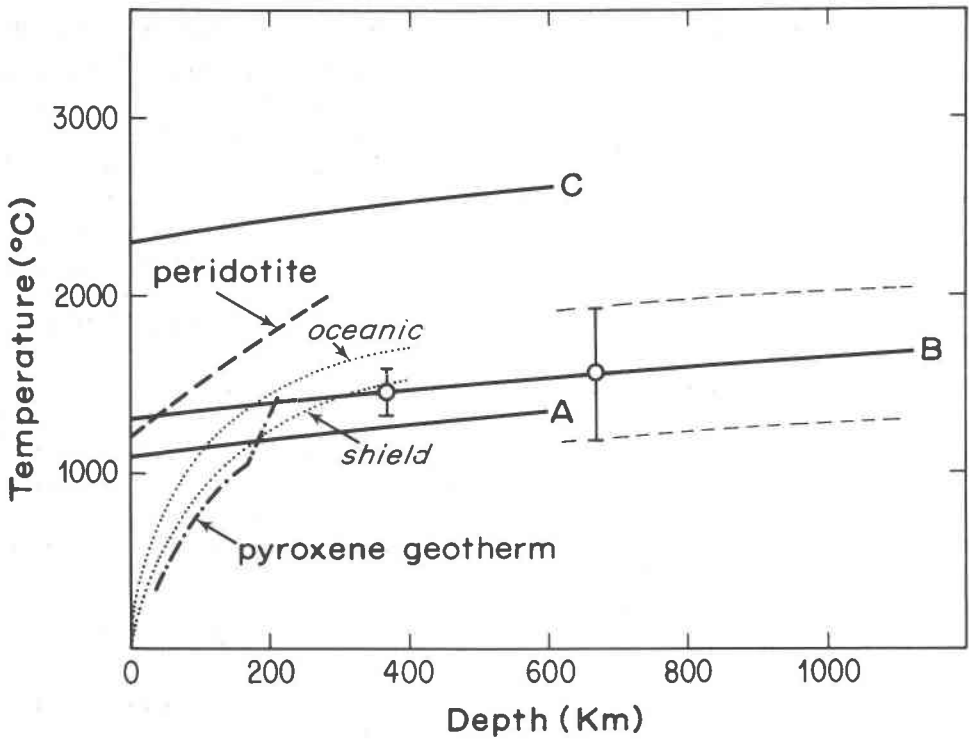

FIG. 7. Adiabatic temperature distribution inferred from compositional models A, B, and C. The respective compositions correspond to $2(Mg_{85}Fe_{15})O+SiO_2$(dunite), $5(Mg_{85}Fe_{15})O+3SiO_2$(peridotite), and $(Mg_{83}Fe_{17})O+SiO_2$(pyroxenite), where (Mg,Fe)O and SiO_2 correspond to magnesiowustite and stishovite. Also shown are the peridotite (dry) melting curve (Kushiro *et al.*, 1968), Clark and Ringwood's (1964) shield and oceanic geotherms, and the pyroxene geotherm (Boyd, 1973) determined from the pressures and temperatures of equilibration of pyroxenes from xenoliths within Lesotho kimberlites. The single point at 370 km and 1450±120°C was determined by Graham (1970) on a basis of the elastic and phase equilibria properties of olivine.

Finally, temperature along the adiabat was determined for each of the compositional models by a direct numerical integration of the above expression, starting at the predetermined zero-pressure temperatures defined by the elastic and density requirements. The resulting adiabatic geotherms for models A, B, and C are shown in Figure 7.

In general, as demonstrated in Figure 7, within the estimates of uncertainty, the adiabatic geotherms for the dunite and peridotite (Models A and B) compositions are consistent with temperature distributions determined for the upper mantle from a variety of independent sources. Moreover, as in the case of the elastic requirements, the pyroxenite model (C) results in a temperature profile which is clearly outside the range of reasonable solutions. The bounds indicated on the peridotite model adiabatic geotherm were determined on a basis of the uncertainties in bulk modulus within the region of interest from the seismic results of Wiggins *et al.* (1973); they provide an appraisal of how well temperature may be assessed in this region of the mantle using composition as a guide. In this regard, if the mantle in the zone of interest is, in fact, compositionally equivalent to dunite–peridotite which has transformed into a mineral assemblage of magnesiowustite and stishovite (plus minor amounts of other phases), then the temperature at the 671 km seismic discontinuity (inversion model B1; Jordan, 1973) is about 1600±400°C.

Conclusions

The following general results regarding the composition and temperature of the mantle immediately below the 650 km seismic discontinuity (approximately 650–1200 km) have accrued from this investigation:

(1) A mixed-oxide assemblage containing (Mg,Fe)O (NaCl structure) and SiO_2 (stishovite) as the primary fractions satisfies the elastic and density requirements of the mantle in the region of interest

when the composition of the mixture is equivalent to a dunite or peridotite; this is not the case if the mixture is pyroxene-rich. This result supports, and is a necessary (but not sufficient) test for the hypothesis that the 650 km seismic discontinuity is the elastic response to a $(Mg,Fe)_2SiO_4$ spinel–mixed-oxide phase transformation (*e.g.* Ming and Bassett, 1975; Kumazawa *et al.*, 1974).

(2) Based on the preferred peridotite interpretation, the Fe/(Mg+Fe) ratio and temperature at 671 km (the depth of the seismic discontinuity for model B1 of Jordan, 1973) are 0.15 ± 0.05 and 1600 ± 400°C.

(3) The temperature gradient in the region of interest appears to lie close to the adiabat; the elastic and density properties of the dunite–peridodite models provide satisfactory correlations to the seismic profiles when they are calculated along adiabatic paths. The temperature uncertainties however, would tend to indicate that this result should be regarded as tentative.

(4) The present investigation, under the constraints imposed by the assumption of composition, does not support a compositional change across the 650 km seismic discontinuity in terms of iron content, where the change in the Fe/(Mg+Fe) ratio is in excess of 0.05 to 0.10; changes smaller than this range are not resolvable by present data and methods. If *substantial* iron enrichment occurs in the lower mantle, relative to the upper mantle, it must take place below 1200 km (the approximate lowest extent of the present range of study).

The question of Fe-enrichment in the lower mantle, especially with respect to sudden changes across phase boundaries, has important implications concerning differentiation processes within the mantle (*e.g.* Press, 1972; Anderson and Jordan, 1970), as well as a significant effect with regard to the stability of convection through the inferred phase transformations in the transition zone (*e.g.* Richter and Johnson, 1974; Sammis, 1975). In view of the estimated uncertainties and assumptions associated with this study, it does not appear likely that an increase in iron content greater than 3 to 6 mole percent could occur across the transition zone; moreover, the range of FeO content allowed by the satisfactory mixed-oxide models (A and B) in the region below the 650 km seismic discontinuity falls between 7 to 14 mole percent. This result is in basic accord with the study of Davies (1974), which was based on a comparison of the density and seismic parameter ϕ requirements of the lower mantle with equations of state for the mixed-oxides and ultramafic rock shock-wave data. The iron enrichment across the transition zone proposed in the studies by Anderson and Jordan (1970), Anderson *et al.* (1971), and Press (1972), covering a range of up to about 7 percent (change in FeO mole percent relative to the upper mantle), is allowed, but not required, by the present results.

Acknowledgments

We wish to thank Professor G. R. Barsch and Dr. M. F. Striefler for providing us with a preprint of their theoretical work on stishovite, and Dr. C. G. Sammis for a preprint of his paper concerning convective stability through phase boundaries. Support for this investigation was provided by NSF Grant No. DES 75-05200.

References

Ahrens, T. J. (1972) The mineralogic distribution of iron in the upper mantle. *Phys. Earth Planet. Int.* **5**, 267–281.

——— (1973) Petrologic properties of the upper 670 km of the Earth's mantle; geophysical implications. *Phys. Earth Planet. Int.* **7**, 167–186.

———, T. Takahashi and G. F. Davis (1970) A proposed equation of state of stishovite. *J. Geophys. Res.* **75**, 310–316.

Akimoto, S. and H. Fujisawa (1968) Olivine–spinel solid solution equilibria in the system Mg_2SiO_4–Fe_2SiO_4. *J. Geophys. Res.*, **73**, 1467–1479.

Anderson, D. L. (1967) Phase changes in the upper mantle. *Science*, **157**, 1165–1173.

——— and T. H. Jordan (1970) The composition of the lower mantle. *Phys. Earth Planet. Int.* **3**, 23–35.

———, C. Sammis and T. Jordan (1971) Composition and evolution of the mantle and core. *Science*, **171**, 1103–1112.

——— and P. Andreatch (1966) Pressure derivatives of elastic constants of single-crystal MgO at 23° and −195.8°C. *J. Am. Ceram. Soc.* **49**, 404–409.

Archambeau, C. B., E. A. Flinn and D. G. Lambert (1969) Fine structure of the upper mantle. *J. Geophys. Res.* **74**, 5825–5867.

Bassett, W. A. and T. Takahashi (1970) Disproportionation of Fe_2SiO_4 to $2FeO + SiO_2$ at high pressure and high temperature (abstract). *Trans. Am. Geophys. Union*, **51**, 828.

Bell, P. M. and H. K. Mao (1975) Geothermometry and geobarometry of the Earth's mantle: an analysis of temperature distribution of the mantle based on the electrical properties of minerals at high pressure (abstr.). Int. Conf. Geothermometry and Geobarometry, The Pennsylvania State University, Oct. 5–10.

Birch, F. (1939) The variation of seismic velocities within a simplified Earth model, in accordance with the theory of finite strain. *Bull. Seism. Soc. Am.* **29**, 463–450.

——— (1952) Elasticity and constitution of the Earth's interior. *J. Geophys. Res.* **57**, 227–286.

Boyd, F. R. (1973) Structure of the upper mantle beneath Lesotho. *Carnegie Inst. Wash. Year Book*, **72**, 431–445.

Chang, E. and E. K. Graham (1975) The elastic constants of cassiterite SnO_2 and their pressure and temperature dependence. *J. Geophys. Res.* **80**, 2595–2599.

Chang, Z. P. and G. R. Barsch (1969) Pressure dependence of the elastic constants of single-crystalline magnesium oxide. *J. Geophys. Res.* **74**, 3291–3294.

Chung, D. H. (1973) Elasticity of high pressure phases (abstr.). *Trans. Am. Geophys. Union*, **54**, 475.

CLARK, S. P. (1966) Handbook of Physical Constants. *Geol. Soc. Am. Mem.* **97.**

——— AND A. E. RINGWOOD (1964) Density distribution and constitution of the mantle. *Rev. Geophys.* **2,** 35–88.

DAVIES, G. F. (1974) Limits on the constitution of the lower mantle. *Geophys. J. R. Astron. Soc.* **38,** 479–504.

DUBA, A. G., H. C. HEARD, A. J. PIWINSKI AND R. N. SHOCK (1975) Electrical conductivity and the geotherm (abstr.). Int. Conf. Geothermometry and Geobarometry, The Pennsylvania State University Oct. 5–10.

FUJISAWA, H. (1968) Temperature and discontinuities in the transition layer with the Earth's mantle: geophysical application of the olivine–spinel transition in the Mg_2SiO_4–Fe_2SiO_4 system. *J. Geophys. Res.* **73,** 3281–3294.

GRAHAM, E. K. (1970) Elasticity and composition of the upper mantle. *Geophys. J. R. Astron. Soc.,* **20,** 285–302.

——— (1973) On the compression of stishovite. *Geophys. J. R. Astron. Soc.* **32,** 15–34.

GREEN, D. H. AND A. E. RINGWOOD (1963) Mineral assemblages in a model mantle composition. *J. Geophys. Res.* **68,** 937–945.

HILL, R. (1952) The elastic behavior of a crystalline aggregate. *Proc. Phys. Soc. London,* **65A,** 439–443.

HOLM, J. L., O. J. KLEPPA AND E. F. WESTRUM (1967) Thermodynamics of polymorphic transformations in silica. Thermal properties from 5 to 1070°K and pressure-temperature stability fields for coesite and stishovite. *Geochim. Cosmochim. Acta,* **31,** 2289–2307.

JOHNSON, L. R. (1967) Array measurements of *P* velocities in the upper mantle. *J. Geophys. Res.* **72,** 6309–6325.

JORDAN, T. H. (1973) *Estimation of the radial variation of seismic velocities and density in the Earth.* Ph.D. Thesis, Calif. Inst. Tech.

KRÖNER, E. (1967) Elastic moduli of perfectly disordered composite materials. *J. Mech. Phys. Solids,* **15,** 319–331.

KUMAZAWA, M., H. SAWAMOTO, E. OHTANI AND K. MASAKI (1974) Post-spinel phase of forsterite and evolution of the Earth's mantle. *Nature,* **247,** 356–358.

KUSHIRO, I., Y. SYONO AND S. AKIMOTO (1968) Melting of a peridotite nodule at high pressures and high water pressures. *J. Geophys. Res.* **73,** 6023–6029.

LAPADU-HARGUES, P. (1953) Sur la composition chimique moyenne des amphiboles. *Bull. Soc. Geol. Fr.* **3,** 153–173.

MACGREGOR, I. D. AND A. R. BASU (1974) Thermal structure of the lithosphere: a petrologic contribution. *Science,* **185,** 1007–1011.

MCGETCHIN, T. R. AND L. T. SILVER (1970) Compositional relations in minerals from kimberlite and related rocks in the Moses Rock Dike, San Juan County, Utah. *Am. Mineral.* **55,** 1738–1771.

MANGHNANI, M. H. (1969) Elastic constants of single-crystal rutile under pressures to 7.5 kilobars. *J. Geophys. Res.* **74,** 4317–4328.

MING, L. C. AND W. A. BASSETT (1975) The postspinel phases in the Mg_2SiO_4–Fe_2SiO_4 system. *Science,* **187,** 66–68.

MITZUTANI, H., Y. HAMANO AND S. AKIMOTO (1972) Elastic wave velocities of polycrystalline stishovite. *J. Geophys. Res.* **77,** 3744–3749.

NIAZI, M. AND D. L. ANDERSON (1965) Upper mantle structure of western North America from apparent velocities of *P* waves. *J. Geophys. Res.* **70,** 4633–4644.

NOCKOLDS, S. R. (1954) Average chemical compositions of some igneous rocks. *Bull. Geol. Soc. Am.* **65,** 1007–1032.

PRESS, F. (1972) The Earth's interior as inferred from a family of models. In E. C. Robertson, Ed., *Nature of the Solid Earth,* McGraw-Hill, New York.

RICHTER, F. M. AND C. E. JOHNSON (1974) Stability of a chemically layered mantle. *J. Geophys. Res.* **79,** 1635–1639.

RINGWOOD, A. E. (1966) The chemical composition and origin of the Earth. In P. M. Hurley, Ed., *Advances in Earth Science,* MIT Press, 287–356.

——— AND A. MAJOR (1966) Synthesis of Mg_2SiO_4–Fe_2SiO_4 spinel solid solutions. *Earth Planet. Sci. Lett.* **1,** 241–245.

ROBIE, R. A. AND D. R. WALDBAUM (1968) Thermodynamic properties of minerals and related substances at 298.15°K (25°C) and one atmosphere (1.013 bars) pressure and high temperatures. *U. S. Geol. Surv. Bull.* **1259.**

SAMMIS, C. G. (1975) The effects of polymorphic phase boundaries on vertical and horizontal motions in the Earth's mantle. *Tectonophysics,* in press.

———, D. L. ANDERSON AND T. JORDAN (1970) Application of isotropic finite strain theory to ultrasonic and seismological data. *J. Geophys. Res.* **75,** 4478–4480.

STRIEFLER, M. E. AND G. R. BARSCH (1975) Elastic and optical properties of stishovite. *J. Geophys. Res.* in press.

THOMSEN, L. (1972) Elasticity of polycrystals and rocks. *J. Geophys. Res.* **77,** 315–327.

TOZER, D. C. (1959) The electrical properties of the Earth's interior. In, L. H. Ahrens, F. Press, K. Rankama, and S. K. Runcorn, Eds., *Physics and Chemistry of the Earth,* **3,** 414–436, Pergamon Press, Oxford.

UFFEN, R. (1952) A method for estimating the melting-point gradient in the Earth's mantle. *Trans. Am. Geophys. Union,* **33,** 893–896.

VICTOR, A. C. AND T. B. DOUGLAS (1963) Thermodynamic properties of magnesium oxide and beryllium oxide from 298° to 1200°K. *J. Res. Natl. Bur. Standards,* **67A,** 325–329.

WANG, C. Y. (1972) Temperature in the lower mantle. *Geophys. J. R. Astron. Soc.,* **27,** 29–36.

WANG, H. AND G. SIMMONS (1973) Elasticity of some mantle crystal structures, 2, Rutile GeO_2. *J. Geophys. Res.* **78,** 1262–1270.

WEAVER, J. S., T. TAKAHASHI AND W. A. BASSETT (1973) Thermal expansion of stishovite (abstr.). *EOS Trans. Am. Geophys. Union,* **54,** 475.

WHITE, G. K. AND O. L. ANDERSON (1966) Grüneisen parameter of magnesium oxide. *J. Appl. Phys.* **37,** 430–432.

WIGGINS, R. A., G. A. MCMECHAN AND M. N. TOKSÖZ (1972) Range of Earth structure non-uniqueness implied by body wave observations. *Rev. Geophys. Space Phys.* **11,** 87–114.